# Effect of plasticity and atmospheric pressure on the formation of donut- and croissantlike buckles

S. Hamade,[1,*] J. Durinck,[1] G. Parry,[2] C. Coupeau,[1] A. Cimetière,[1] J. Grilhé,[1] and J. Colin[1]

[1]*Institut P', Université de Poitiers, ENSMA, SP2MI-Téléport 2, 86962 Futuroscope-Chasseneuil cedex, France*

[2]*Science et Ingénierie des Matériaux et Procédés, Université de Grenoble, 1130 rue de la Piscine, BP 75, 38402 St Martin d'Heres cedex, France*

(Received 17 October 2014; revised manuscript received 25 November 2014; published 30 January 2015)

The formation of donut- and croissantlike buckles has been observed onto the free surface of gold thin films deposited on silicon substrates. Numerical simulations clearly evidence that the coupling effect between the atmospheric pressure acting on the free surface and the plastic folding of the ductile film is responsible for the circular blister destabilization and the formation of the donut- and croissantlike buckling patterns.

DOI: 10.1103/PhysRevE.91.012410 PACS number(s): 68.55.−a, 46.32.+x, 62.25.−g

## I. INTRODUCTION

The control of the mechanical properties of multilayered structures is a long-standing problem that has been intensively studied from both experimental and theoretical point of view because of the numerous applications of such patterns in electronic and optoelectronic devices [1]. The delamination and buckling of thin films deposited on substrates have been investigated, for example, when the films are internally strained due to lattice and/or thermal expansion coefficient mismatches between the film and the substrate [2–4]. In the framework of the Föppl von Kármán theory of thin plates [5,6], different structures observed at the nano- (and meso-) scales with the help of an atomic force (optical) microscope have been thus characterized such as circular blisters and straight-sided and telephone cord buckles. The critical stress beyond which the straight-sided blisters appear has been determined, for example, as well as the film profiles after buckling. Likewise, the effects of the substrate elasticity and stress anisotropy have been characterized, and a stability diagram has been provided for the formation of the circular blisters and straight-sided and telephone cord buckles [7]. The effect of the thin film plasticity then has been considered, and the formation of folded structures observed on the surface of ductile gold thin films has been explained [8,9]. Recently the effect of overpressure between the upper and lower surfaces of the films has been investigated on the morphological evolution of buckles generated by internal strains [10]. It has been found that this overpressure is responsible for the partial redeposition of the buckled part of the films [11]. An experimental study of the buckling of nickel thin films deposited on polycarbonate substrates has also evidenced a pressure mismatch between the outer free surface of the film and the inner film-substrate interface. The presence of vacuum has thus been deduced between the film and its substrate [12].

In this paper the combined effects of internal stress, atmospheric pressure applied onto the film free surface, and thin film plasticity have been investigated on the buckling patterns through finite element simulations. The formation of donut- and croissantlike morphologies experimentally observed on the surface of a gold thin film has been explained in the framework of the continuum nonlinear mechanics.

*sami.hamade@univ-poitiers.fr

## II. EXPERIMENTAL OBSERVATIONS

Gold films have been first deposited by sputtering methods on silicon wafers. The physical vapor deposition (PVD) technique leads to homogeneous films with well-defined constant thicknesses. The thickness of the gold films has been determined by DEKTAK mechanical profilometry to be equal to $h = 630$ nm. It can be seen in Fig. 1(a) that after removing the specimens from the deposition chamber, the thin films exhibit a plethora of buckling structures, among which one can cite the circular blisters and croissantlike and donutlike buckles. A correlation between the dimensions and the shapes of such structures then has been established in Fig. 1(b). It can be observed that circular buckles develop for the smallest delamination area at the interface (region A), while croissant- and donutlike shapes appear for the intermediate and largest areas corresponding to regions B and C, respectively. Two critical widths have thus been determined, $2b_c^1 \sim 71$ $\mu$m and $2b_c^2 \sim 127$ $\mu$m, that characterize the blister to croissantlike buckle and the croissant- to donutlike buckle transitions, respectively. It can be emphasized at this point that these transitions are supposed to depend on the buckle plastic deformation and the local stress state in the film. Since these parameters may vary in our experimental conditions for a given sample, a few of circular blisters and croissantlike buckles have been thus experimentally observed for similar widths. It can also be underlined that such large buckling structures (reaching sometimes 200 $\mu$m wide) are rarely mentioned in the literature, since the full delamination of the film-substrate interface usually occurs. Evidence of thin film plasticity is provided in Fig. 1(c). Indeed, fine surface features are observed on the flat part of the croissantlike structures as well as a superposition of several circular buckles. These observations can be ascribed to plastic events already observed in similar systems at the circumference of buckles [8,9] and support the idea of a complete initial circular delamination at the film-substrate interface before the partial redeposition takes place, leading to croissant- or donutlike structures.

## III. MODELING AND DISCUSSION

In order to describe the effect of pressure and plasticity on the postbuckling regime of a circular blister, a geometrically nonlinear plate model is used in order to describe the thin film. The substrate surface is represented by a rigid plane

 

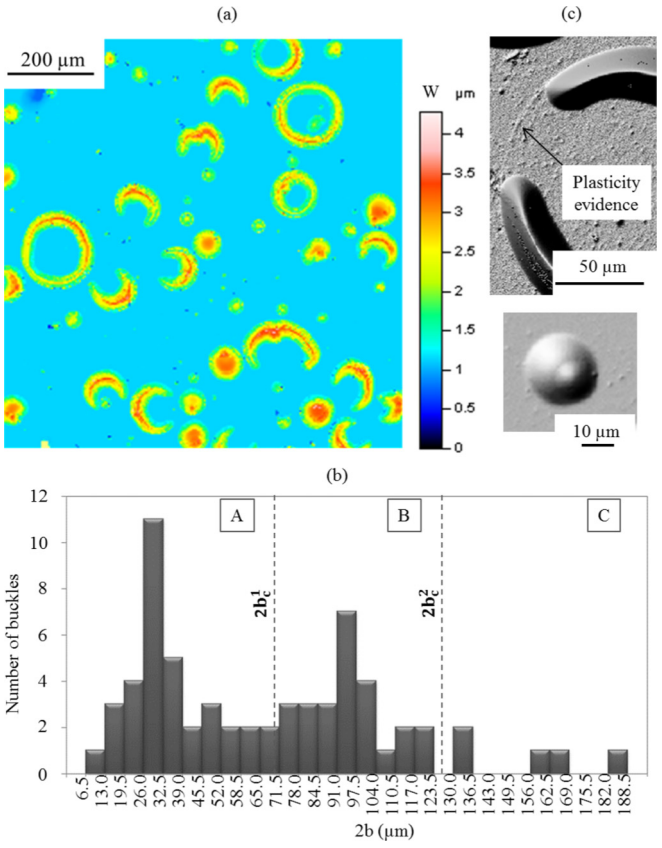


FIG. 1. (Color online) Optical observations of the surface of a gold thin film of thickness $h = 630\ nm$ after its deposition on a silicon substrate. (a) Panoramic view of the surface obtained by white light interferometer. (b) Statistical description of the different morphologies of buckles as a function of diameter $2b$. Three regions A, B, and C have been identified where circular blisters, croissantlike and donutlike buckles develop, respectively. (c) Experimental evidences of thin film plasticity: fine surface features on the flat part of a croissantlike structure and buckle superposition with plastic folding at the buckle circumferences.

forbidding the displacement of the plate in the lower half-space (unilateral contact condition), and as a consequence the elastic deformation of the substrate is not considered.

The plate is a circular domain $\Omega$ with center $O$ and radius $b$ and is originally in a planar state with its midplane located at the substrate surface [see Fig. 2(a)]. Let us denote by $(Oz)$ the direction of the normal to the substrate surface. For convenience, a cylindrical coordinate system of axis $(Oz)$ is used to describe the kinematic of the plate, and $u(r,\theta), v(r,\theta)$, and $w(r,\theta)$ are the displacement components along the axes parallel to $\vec{e}_r$, $\vec{e}_\theta$, and $\vec{e}_z$, respectively, for any point $M(r,\theta)$ of the midplane. The boundary conditions are imposed along the edge $\partial\Omega$ of the plate, $\partial\Omega = \{M(b,\theta), 0 \leqslant \theta < 2\pi\}$, such that

$$\forall M \in \partial\Omega, u(M) = v(M) = w(M) = 0, \quad \frac{\partial w}{\partial r}(M) = \beta, \qquad (1)$$

where $\beta$ is an angle defined in order to mimic the plastic folding. The various buckling patterns are characterized by large values of the out-of-plane displacement component $w(r,\theta)$ such that the calculations must be carried out within

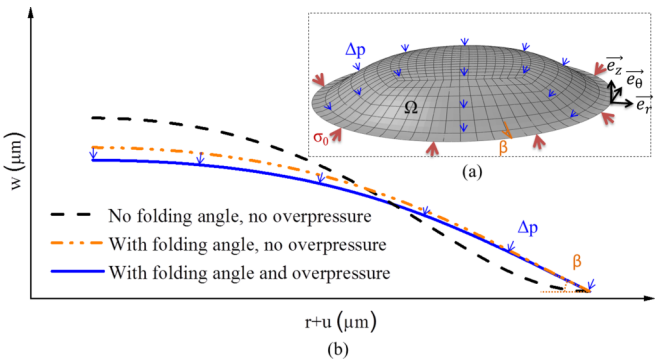


FIG. 2. (Color online) (a) Schematic representation of the meshed circular buckle with a folding angle $\beta$ used in the FEM simulations. A radial compression stress $\sigma_0$ and an external overpressure $\Delta p$ are applied to the structure. (b) Sketch of the effect of the overpressure and plastic folding angle onto the buckle morphology.

the framework of large displacement hypothesis using the Green-Lagrange strain tensor. The plate is submitted to three loading steps:

*Step 1.* Application of the internal stress.

The parameter $\beta$ is set to zero, yielding to the classical clamped edge conditions usually invoked for the buckling of elastic thin films on rigid substrates [2]. An internal compressive stress is introduced in the film as $\sigma_{rr} = \sigma_{\theta\theta} = -E_f/(1-\nu_f)\epsilon_0 = -\sigma_0$ and $\sigma_{r\theta} = 0$, with $\epsilon_0$ a positive and constant eigenstrain, and $E_f$ and $\nu_f$ the Young's modulus and Poisson's ratio of the film, respectively. For a gold thin film, one will take in the following: $E_f = 79$ GPa and $\nu_f = 0.44$. At this point, the obtained solution corresponds to the classical circular blister [2] [see the dashed black line in Fig. 2(b)]. Note that the eigenstrain is maintained during the next steps.

*Step 2.* Mimicking the plastic folding.

In order to mimic the plastic folding at the buckle edge, a folding angle $\beta$ has been imposed all along the circumference $\partial\Omega$ of the clamped buckle. This angle whose value will be specified later is maintained during the procedure. At this point, it can be underlined that the shape of the blisters remains circular, with a smooth change of geometry [see the dashed-double dotted orange line in Fig. 2(b)].

*Step 3.* Application of the pressure.

A uniform overpressure $\Delta p = p_e - p_i$ is applied, with $p_e$ and $p_i$ the pressures applied onto the upper and lower surfaces of the buckled film, respectively. The equilibrium can be dramatically modified by this loading, leading to secondary buckling equilibria quite remote from the original circular shape in the postcritical regime [see the solid blue line in Fig. 2(b)].

In order to carry out these nonlinear calculations, finite element simulations have been performed using the software ABAQUS [13]. An implicit scheme has been selected. Quadrilateral shell elements have been used to mesh the film. The element sizes have been chosen in such a way that a minimum of 28 elements are considered into the film along the diameter.

In the following, the results of the calculation have been rationalized using nondimensional parameters for the loading.

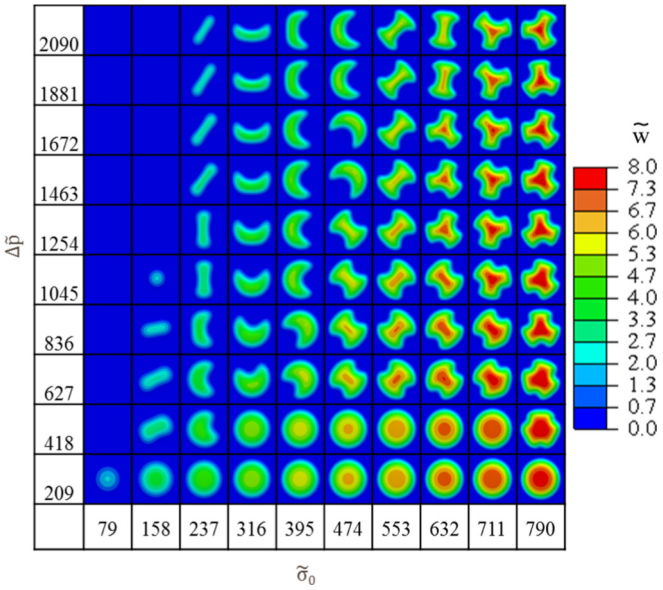


FIG. 3. (Color online) Shape diagram in the $(\tilde{\sigma}_0, \Delta\tilde{p})$ plane for the buckle without any plasticity, i.e., for $\beta = 0^\circ$. The color scale for the normalized out-of-plane displacement $\tilde{w}$ of the film is also displayed.

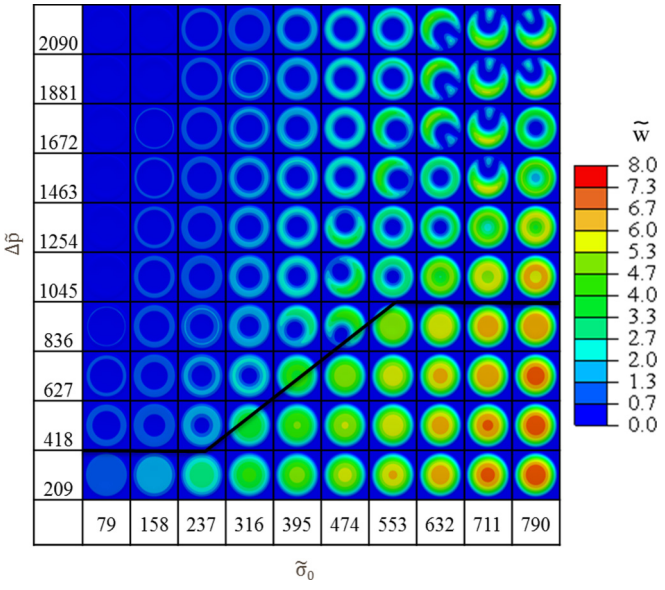


FIG. 4. (Color online) Shape diagram in the $(\tilde{\sigma}_0, \Delta\tilde{p})$ plane for the buckles undergoing plastic folding characterized by a folding angle $\beta = 5^\circ$. The values of the out-of-plane displacement are presented on the color scale. The full black line corresponds to the boundary between the regime of formation of circular blisters and the regime of formation of donut- and croissantlike buckles

Hence, $\tilde{\sigma}_0$ and $\Delta\tilde{p}$ have been defined as

$$\tilde{\sigma}_0 = \frac{12\sigma_0}{\tilde{E}_f}\frac{1}{\tilde{h}^2}, \quad \Delta\tilde{p} = \frac{12\Delta p}{\tilde{E}_f}\frac{1}{\tilde{h}^4}, \tag{2}$$

with $\tilde{h} = h/b$, $\tilde{E}_f = E_f/(1-\nu_f^2)$ and $b$ the radius of the delaminated interface. Before applying loading steps 1 and 3, an initial modification of the out-of-plane displacement $\tilde{w} = w/h$ has been applied to a circular blister of width $2b$ and maximum out-of-plane displacement $10^{-4}b$ in order to facilitate the thin film evolution. For each stress state of the film ($\tilde{\sigma_0}$, $\beta$, $\Delta\tilde{p}$), five different perturbations of the initial displacement $\tilde{w}$ of the circular blister, corresponding to the first five buckling modes of the film, have been tested. The most stable equilibrium pattern is then selected for a given loading state ($\tilde{\sigma_0}$, $\beta$, $\Delta\tilde{p}$) which corresponds to the structure of minimum potential energy.

The buckling has been investigated considering first that no plasticity occurs in the film in order to focus on the pressure effect on buckling patterns. The calculations have been thus carried out ignoring loading step 2 described above and keeping $\beta = 0$. A shape diagram for the buckles has been displayed in Fig. 3 in the ($\tilde{\sigma_0}$, $\Delta\tilde{p}$) plane, where the values of the out-of-plane displacement of the film $\tilde{w}$ have been added on a color scale. It can be noticed that the dimensionless value of the overpressure $\Delta\tilde{p} = 2090$ would correspond to the application of the atmospheric pressure on the free surface of the considered gold thin film ($h = 630$ nm), the internal pressure between the film and the substrate being zero in the vacuum hypothesis [12]. It is clearly evidenced in Fig. 3 that the coupled effect of $\Delta\tilde{p}$ and $\tilde{\sigma_0}$ is to destabilize the circular blisters and to facilitate, as $\Delta\tilde{p}$ increases, the formation of a plethora of buckle morphologies such as croissantlike, two- and three-lobe structures. However, it appears that the donutlike morphology observed onto the surface of the gold thin film does not emerge from this first numerical analysis. The next step of this present paper has been thus to consider the effect of plasticity of the ductile thin film. To do so, it is assumed that, following previous experimental studies [9], the plasticity of the ductile film results in the formation of a plastic folding characterized by an angle taken to be constant all along the circumference of the buckle, $\beta = 5^\circ$. This value of $\beta$ angle will be justified later.

A new shape diagram has been then constructed in the $(\tilde{\sigma}_0, \Delta\tilde{p})$ plane assuming $\beta = 5^\circ$ and using the same procedure as the one already described in the plasticity free case. This new diagram taking into account the thin film folding is presented in Fig. 4. It can be observed that the main effect of folding is to stabilize the buckle circumference in such a way that only two shapes promoted by the overpressure appear to be selected: the donut- and croissantlike morphologies. Indeed, when $\tilde{\sigma_0}$ is high and $\Delta\tilde{p}$ is small, the circular blister pattern is expected, otherwise the donut- and croissantlike patterns dominate. The boundary characterizing the transition between these two regimes of buckles has been superimposed in Fig. 4 (see the full dark line).

In order to characterize the influence of the atmospheric pressure on buckling, the previous results obtained by means of finite element simulations have been analyzed in the case of the gold thin films deposited on silicon substrates firstly presented that are lying in the air condition. An internal compressive stress $\sigma_0 = 321$ MPa and a folding angle $\beta = 5^\circ$ have been considered. Taking an overpressure $\Delta p = 0.1$ MPa (or $\Delta\tilde{p} = 2090$) corresponding to the atmospheric overpressure, it can be observed in Fig. 5 that the different buckle morphologies observed at different delamination widths $2b$ on the surface of the gold thin film, i.e., a circular blister for $2b = 40$ $\mu$m, a croissantlike buckle for $2b = 118$ $\mu$m, and a donutlike buckle

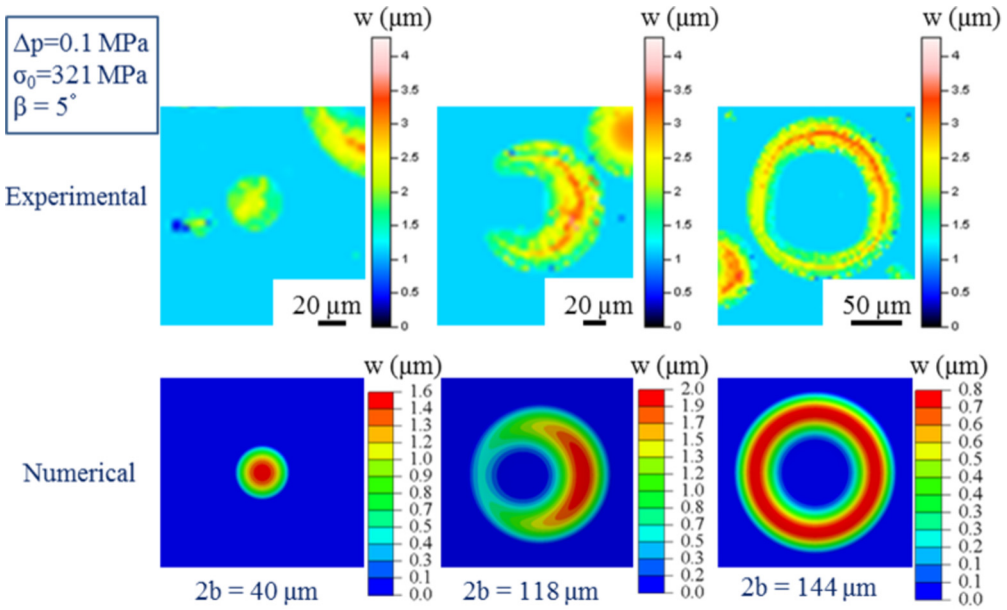


FIG. 5. (Color online) Comparison between three experimental and numerical shapes of the buckles for an atmospheric overpressure $\Delta p = 0.1$ MPa, an internal radial compression stress $\sigma_0 = 321$ MPa, and a folding angle $\beta = 5^\circ$.

for $2b = 144$ $\mu$m, have been also obtained in our simulations considering the overpressure and thin film plasticity.

The numerical value $\beta = 5^\circ$ of the folding angle has been confirmed through finite element simulations where the film has been meshed with solid elements and the plasticity has been described in terms of material constitutive relation instead of geometrical folding angle. The effect of pressure and plasticity on the postbuckling regime of a circular blister is described by a geometrically nonlinear plate modeling the thin film. The circular domain $\Omega$ of the plate is replaced by a cylindrical domain $D$ with a thickness $h = 630$ nm (see Fig. 6). The base of the cylinder has a center $O$ and a radius $2b$ and is located at the substrate surface. As for the model with shell elements with a folding angle, the substrate surface is considered to be a rigid plane forbidding the displacement of the plate into the lower half-space. The coordinate system is cylindrical, with $(Oz)$ the vertical axis. The displacement components are $u(r,\theta,z)$,$v(r,\theta,z)$, and $w(r,\theta,z)$ along the axes parallel to $\vec{e}_r$, $\vec{e}_\theta$, and $\vec{e}_z$, respectively, for any point

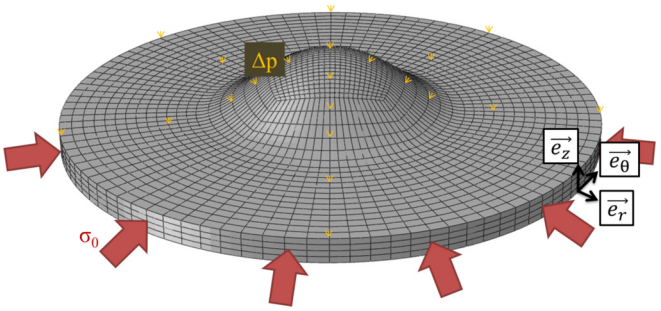


FIG. 6. (Color online) Schematic representation of the meshed film of domain $D$ used in the second model of FEM simulations. A radial compression stress $\sigma_0$ and an external overpressure $\Delta p$ are applied to the structure.

$M(r,\theta,z)$ of the plate. The first boundary condition is a clamped surface condition along the lateral surface $\partial D_1$ of the plate, $\partial D_1 = \{M(r,\theta,z), r = 2b, 0 \leqslant \theta < 2\pi, 0 \leqslant z \leqslant h\}$. The second boundary condition acts on the bottom surface $\partial D_2 = \{M(r,\theta,z), b \leqslant r \leqslant 2b, 0 \leqslant \theta < 2\pi, z = 0\}$ such that

$$\forall M \in \partial D_2, \quad u(M) = v(M) = w(M) = 0, \tag{3}$$

the film being bonded to the substrate in this area. The delaminated part of the film that can buckle is then limited to the subdomain $D_b$ of the plate such as $D_b = \{M(r,\theta,z), 0 \leqslant r \leqslant b, 0 \leqslant \theta < 2\pi, 0 \leqslant z \leqslant h\}$, with unilateral contact conditions for the bottom surface of the film. The material constitutive relation used to describe the uniform plastic deformation of the film is a power law strain hardening equation proposed by Ludwik [14]:

$$\forall \sigma \geqslant \sigma_y, \quad \sigma = \sigma_y + K\epsilon_p^n, \tag{4}$$

where $\sigma$ and $\epsilon_p$ are the true stress and plastic strain, respectively, with the initial yield stress $\sigma_y = 95$ MPa when the plastic strain $\epsilon_p$ is zero, $n = 0.25$ the strain hardening exponent, and $K = 134.4$ MPa the strength coefficient [15]. The Young's modulus and Poisson's ratio of the film are $E_f = 79$ GPa and $\nu_f = 0.44$, respectively.

The plate is submitted to two loading steps:

*Step 1.* Application of the internal stress.

An internal compressive stress is introduced in the film as: $\sigma_{rr} = \sigma_{\theta\theta} = -\sigma_0$. At this point, the obtained solution corresponds to the classical circular blister [2]. Note that the eigenstrain is maintained during the next step.

*Step 2.* Application of the pressure.

A uniform overpressure $\Delta p$ is applied.

Quadrilateral solid elements have been used to mesh the film. The elements size have been chosen in such a way that a minimum of 28 elements are considered into the subdomain

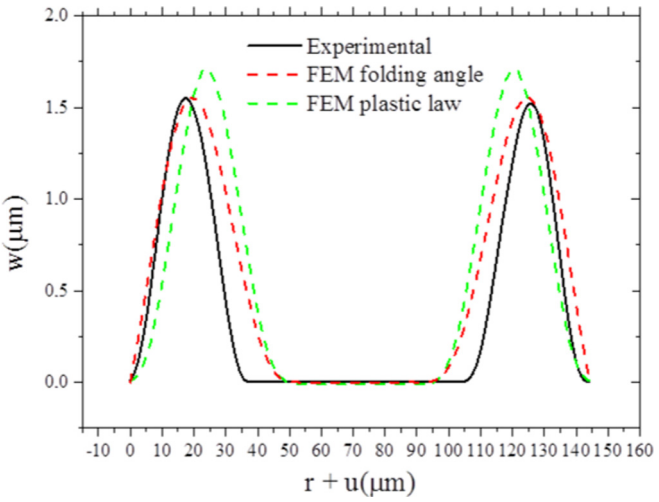


FIG. 7. (Color online) Comparison between the profiles of a donutlike buckle obtained by experimental observations, finite element simulations with an imposed plastic folding angle and finite element simulations with a plastic material law, taking an overpressure of the order of the atmospheric pressure $\Delta p = 0.1$ MPa, an internal radial compression stress $\sigma_0 = 321$ MPa and a folding angle $\beta = 5^\circ$.

$D_b$ of the film along the diameter and four elements along the film thickness (see Fig. 6). An internal compressive stress $\sigma_0 = 321$ MPa has been considered. The different profiles of the donutlike buckle derived from experimental observations, finite element simulations in the elasticity framework with an imposed plastic folding angle, and finite element simulations with a plastic material law (without any given value for the folding angle) have been plotted in Fig. 7. It is evidenced in this Fig. 7 that both simulation profiles fit with the experimental one, justifying thus the choice of the value of the angle $\beta = 5^\circ$ and internal stress $\sigma_0 = 321$ MPa used in our work.

Finally, the buckles corresponding to the minimum energy have been determined in Fig. 8 as a function of the increasing delamination width $2b$. To do so, finite element calculations with shell elements have been performed as in the first part of this section. In the case where an overpressure of the order of the atmospheric pressure is acting on the surface of the film, with an internal biaxial stress $\sigma_0 = 321$ MPa and a folding angle $\beta = 5^\circ$, three separated regions labeled A, B, and C have been identified in Fig. 8 in good agreement with

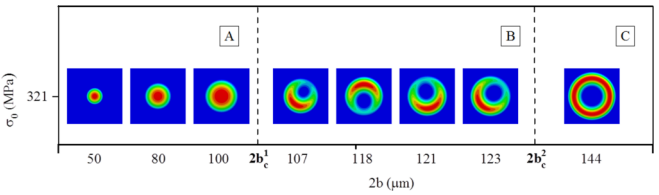


FIG. 8. (Color online) Buckle patterns as a function of the increasing delamination width $2b$. Finite elements results for a fixed atmospheric pressure $\Delta p = 0.1$ MPa, an internal compression stress $\sigma_0 = 321$ MPa, and a folding angle $\beta = 5^\circ$.

the statistical diagram derived from the experimental observations presented in Fig. 1(b). In particular, the two critical widths $2b_c^1 \sim 104$ $\mu$m and $2b_c^2 \sim 134$ $\mu$m characterizing the blister to croissantlike buckle and the croissant to donutlike buckle transitions derived from the simulations are of the good order of magnitude with the experimental ones. It can also be underlined that the residual plasticity traces experimentally observed in Fig. 1(c) have been obtained in the simulations of the croissantlike buckles for $b \in [b_c^1, b_c^2]$, where the vertical deformation located near the circumference of the former circular blisters is still present.

## IV. CONCLUSION

In this paper the coupled effects of pressure and thin film plasticity have been characterized on the buckling patterns appearing onto the surface of thin films deposited on substrates, and a shape diagram has been derived for the buckles by means of finite element simulations. It is clearly evidenced that an overpressure of the order of the atmospheric pressure and a plastic folding along the circumference of the buckles can explain the formation of the donut- and croissantlike buckles observed for different widths of interface delamination in the case of ductile gold thin films. It is believed that a dynamic study of the evolution of the buckling structure under pressure and compression stress should now be performed considering the interaction between the delamination process and buckling phenomenon in order to get a more complete overview of the thin film aging.

## ACKNOWLEDGMENT

This work pertains to the French Government program LABEX INTERACTIFS (Investissements d'Avenir, ANR-11-LABX-0017-01).

[1] L. B. Freund and S. Suresh, *Thin Film Materials: Stress, Defect Formation and Surface Evolution* (Cambridge University Press, Cambridge, 2003), p. 355.

[2] J. W. Hutchinson and Z. Suo, Mixed mode cracking in layered materials, Adv. Appl. Mech **29**, 63 (1992).

[3] M. W. Moon, H. M. Jensen, J. W. Hutchinson, K. H. Oh, and A. G. Evans, The characterization of telephone cord buckling of compressed thin films on substrates, J. Mech. Phys. Solid **50**, 2355 (2002).

[4] B. Audoly, Stability of straight delamination blisters, Phys. Rev. Lett **83**, 4124 (1999).

[5] A. Föppl, *Vorlesungen über Technische Mechanik* (Springer, Vienna, 1907), Vol. 5, P. 132.

[6] T. V. Kármán, *Encyklopädie der Mathematischen Wissenschaften* (B. G. Teubner, Leipzig, 1910), IV/4C, p. 311.

[7] G. Parry, A. Cimetière, C. Coupeau, J. Colin, and J. Grilhé, Stability diagram of unilateral buckling patterns of strip-delaminated films, Phys. Rev. E **74**, 066601 (2006).

[8] F. Foucher, C. Coupeau, J. Colin, A. Cimetière, and J. Grilhé, How does crystalline substrate plasticity modify thin film buckling?, Phys. Rev. Lett **97**, 096101 (2006).

[9] J. Colin, C. Coupeau, and J. Grilhé, Plastic folding of buckling structures, Phys. Rev. Lett **99**, 046101 (2007).

[10] E. Dion, J. Grilhé, J. Colin, and C. Coupeau, Buckling of stressed and pressurized thin films on substrates, J. Appl. Mech **77**, 041012 (2010).

[11] J. Colin, C. Coupeau, J. Durinck, A. Cimetière, and J. Grilhé, Redeposition of a straight-sided buckle under pressure, Phys. Rev. E **89**, 032410 (2014).

[12] C. Coupeau, J. Grilhé, E. Dion, L. Dantes de Morais, and J. Colin, Evidence of vacuum between buckled films and their substrates, Thin Solid Films **518**, 5233 (2010).

[13] ABAQUS Manuals Collection, Dassault Systèmes Simulia-Corp., Providence, RI, USA (2012).

[14] P. Ludwik, *Elemente der Technologischen Mechanik* (Verlag von Julius Springer, Berlin, 1909), p. 32.

[15] M. F. Ashby and D. R. H. Jones, *Engineering Materials I* (Butterworth Heinemann, Oxford, 1996).